Biosensors and Bioelectronics 61 (2014) 519–525

Contents lists available at ScienceDirect

Biosensors and Bioelectronics

journal homepage: www.elsevier.com/locate/bios

# Mesoporous carbon nitride based biosensor for highly sensitive and selective analysis of phenol and catechol in compost bioremediation

Yaoyu Zhou [a,b], Lin Tang [a,b,*], Guangming Zeng [a,b,*], Jun Chen [a,b], Ye Cai [a,b], Yi Zhang [a,b], Guide Yang [a,b], Yuanyuan Liu [a,b], Chen Zhang [a,b], Wangwang Tang [a,b]

[a] College of Environmental Science and Engineering, Hunan University, Changsha 410082, China
[b] Key Laboratory of Environmental Biology and Pollution Control, Hunan University, Ministry of Education, Changsha 410082, China

ARTICLE INFO

*Article history:*
Received 19 March 2014
Received in revised form
23 May 2014
Accepted 29 May 2014
Available online 8 June 2014

*Keywords:*
Mesoporous carbon nitride
Biosensor
Phenol
Catechol
Compost bioremediation

ABSTRACT

Herein, we reported here a promising biosensor by taking advantage of the unique ordered mesoporous carbon nitride material (MCN) to convert the recognition information into a detectable signal with enzyme firstly, which could realize the sensitive, especially, selective detection of catechol and phenol in compost bioremediation samples. The mechanism including the MCN based on electrochemical, biosensor assembly, enzyme immobilization, and enzyme kinetics (elucidating the lower detection limit, different linear range and sensitivity) was discussed in detail. Under optimal conditions, GCE/MCN/Tyr biosensor was evaluated by chronoamperometry measurements and the reduction current of phenol and catechol was proportional to their concentration in the range of $5.00\times10^{-8}$–$9.50\times10^{-6}$ M and $5.00\times10^{-8}$–$1.25\times10^{-5}$ M with a correlation coefficient of 0.9991 and 0.9881, respectively. The detection limits of catechol and phenol were 10.24 nM and 15.00 nM (S/N=3), respectively. Besides, the data obtained from interference experiments indicated that the biosensor had good specificity. All the results showed that this material is suitable for load enzyme and applied to the biosensor due to the proposed biosensor exhibited improved analytical performances in terms of the detection limit and specificity, provided a powerful tool for rapid, sensitive, especially, selective monitoring of catechol and phenol simultaneously. Moreover, the obtained results may open the way to other MCN–enzyme applications in the environmental field.



## 1. Introduction

Catechol and phenol pose a serious threat to human and environmental health worldwide. Such compounds mostly originate from various agricultural, chemicals and industrial byproducts, including wood preservatives, dyes, paper, herbicides, petrochemical, and textile industries and the partial degradation of phenoxy contaminants in remediation processes (Švitel and Miertuš, 1998; Wang et al., 2013). The toxicity of such compounds generated from bioremediation, such as composting, can also bring on undesirable ecological effects and seriously damage removal efficiencies (Tang et al., 2008). Catechol can affect the nerve center system of human beings, inhibit DNA replication, and lead to chromosomal aberration (Topping et al., 2007). Phenol, a compound regarded as a priority contaminant by the U.S. Environmental Protection Agency, has caused much concern because of their toxicity and possible accumulation in the environment. With the increasing application of composting technology in disposal of municipal solid waste, catechol and phenol are generally direct pollutants or by-products of the aromatic pollutant biodegradation and of great significance for control in composting technology (Canofeni et al., 1994; Tang et al., 2008). In this regard, it is highly necessary and urgent to develop a facile, robust, and real-time method for the determination of catechol and phenol in compost bioremediation of municipal solid waste with high sensitivity, especially, selectivity.

Selectivity is of great importance to be considered for biosensors detecting phenols derivates in compost systems because there exist a variety of organic compounds and heavy metals. Although a great many research have shown the effect of interferents, such as heavy metals, benzaldehyde, benzylalcohol on the tyrosinase biosensor to the best of our knowledge, hydroquinone, an indirect substrate of tyrosinase, as an interferent of catechol and phenol detected by tyrosinase biosensors has not been studied. What is more, there are few articles reporting the mutual interference between them. In fact, in order to apply the biosensor to real samples, it is necessary to study the interference effect of hydroquinone for the biosensor because catechol and hydroquinone have similar structures and properties, and they usually coexist in

* Corresponding authors at: College of Environmental Science and Engineering, Hunan University, Changsha 410082, China. Tel./fax: +86 731 88822778.
*E-mail addresses:* tanglin@hnu.edu.cn (L. Tang), zgming@hnu.edu.cn (G. Zeng).

http://dx.doi.org/10.1016/j.bios.2014.05.063
0956-5663/

the environment. Therefore, searching for the interference effect between catechol and phenol, and other interferent especially hydroquinone, is of great significance in order to improve the potential of practical application of the biosensor.

The traditional techniques for catechol and phenol detection are mainly focused on high performance liquid chromatography (HPLC), spectrophotometry and gas chromatography, which achieve the excellent performances at the expense of time, cost and tedious procedures for sample pretreatment or preconcentration (Ramiz et al., 2012). Hence, many efforts have been devoted to the development of simple and effective analytical methods for the determination of catechol and phenol. Electrochemical sensors provide simple, sensitive and convenient tools for this purpose but the characters such as sensitivity, repeatability and reproducibility especially, specificity need to be improved (Apetrei et al., 2011; Zhang et al., 2011).

To overcome these limitations, the past years have witnessed great progress in electrochemical enzyme-based biosensors which constitute promising technology for the in situ monitoring of catechol and phenol. In particular, chronoamperometry biosensors based on tyrosinase (Tyr) and polyphenol oxidase (PPO) have been proved to be sensitive and convenient for the determination of phenols (Švitel and Miertuš, 1998; Fusco et al., 2010). The tyrosinase biosensor is usually developed based on monitoring the reduction signal of the quinine species, which is generated by the catalysis of tyrosinase in the presence of molecular oxygen. Therefore, the appropriate immobilization of the enzyme on the electrode surface is considered a key step in the development of tyrosinase biosensors for phenols determination (Švitel and Miertuš, 1998; Lu et al., 2010). On one hand, tyrosinase have been immobilized using a range of techniques including immobilization onto carbonaceous electrodes via the physical adsorption (Peralta-Zamora et al., 2003), layer-by-layer (LbL) and the Langmuir–Blodgett (LB) techniques (Caseli et al., 2009), the cross-linking step by glutaraldehyde (Zhao et al., 2009) and immobilization in polymeric matrixes (Yildiz et al., 2006). On the other hand, various supporting materials have been successfully used to immobilize tyrosinase (Tyr) on the electrode recently. Nanomaterials are regarded as ideal candidates facilitating efficient signal transduction and molecular recognition during the detection process resulting from their unique structural and electronic features. To date, various nanomaterials, such as graphene-silk peptide (Gr–SP) nanosheets (Qu et al., 2013), ZnO nanoparticles (Li et al., 2006), calcium carbonate nanoparticles (Shan et al., 2007), gold nanoparticles (Au-NP) (Song et al., 2011), hydroxyapatite nanoparticles (Lu et al., 2010), Bi nanoparticles (Carmen et al., 2013), multiwalled carbon nanotube (MWNTs) (Tsai and Chiu, 2007), carbon nanotubes-chitosan (CNTs–CS) (Liu et al., 2006), have been successfully exploited for phenols quantification relying on different transduction schemes, offering promising advantages in terms of feasible miniaturization, cost-effectiveness, sensitivity (even in the nM level), and analysis time in comparison with routine biosensors.

Moreover, searching for new simple, reliable and inexpensive schemes to immobilize tyrosinase is also of considerable interest. Alternatively, ordered mesoporous carbon (OMC) is a kind of novel advanced carbon material. Since the discovery of OMC in 1999 (Ryoo et al., 1999), increasing attention has been focused on the fundamental research and applications of OMC owing to their extremely uniform pore structure, large pore volume, high specific surface area, tunable pore size distribution, chemical inertness and biocompatibility (Zhou et al., 2008). Due to the ability of fast electron transfer, avoiding surface fouling and excellent electrocatalytic activity, OMC has been widely used in sensing (Zhou et al., 2008; Liu et al., 2010), bioreactor construction (Hartmann, 2005), etc. The improved electrochemical reactivity of OMC suggests that it will be a promising alternative candidate for electrode materials. Recently, carbon nitride (CN) is a well known and fascinating material that has attracted worldwide attention because the incorporation of nitrogen atoms in the carbon nanostructure can form unique combination of properties, such as extreme hardness, low density, semiconductivity, biocompatibility, special optical features, energy-storage capacity, gas adsorption capacity, and the presence of basic sites (Vinu et al., 2005). And carbon nitride, especially, ordered mesoporous carbon nitride material, designated as MCN, with large surface areas, small particle sizes, and large surface areas, small particle sizes and tunable pore diameters promise access toan even wider range of applications, such as catalyst (Wu et al., 2012; Xin et al., 2009), supercapacitors (Wei et al., 2013), rechargeable lithium–air battery (Lu et al., 2012), and adsorbent (Park et al., 2011). However, using MCN to construct the biosensor with the immobilized enzyme has rarely been reported. In fact, MCN combines the advantages of both parts (OMC and CN), then strengthens the features, including higher affinity for bioactivator, larger bioactivity after entrapment procedure because of the CN matrix, and faster electron transfer between bioactivator and MCN-sensing sites because of the $\pi$–$\pi^*$ electronic transition in the MCN (Vinu et al., 2005). These properties of MCN provide an excellent platform for enzyme and protein immobilizations and faster electron transfer as well. Herein, such MCN was exploited as a transducer to convert the recognition information into a detectable signal with enzyme.

In the current study, we proposed the development of a chronoamperometry MCN/Tyr-based biosensor, which has not been reported so far. The resulting MCN/Tyr-based biosensor exhibited high specificity toward phenol and catechol in compost samples. This method enabled the development of fast and inexpensive on-line monitoring systems in municipal solid waste compost bioremediation. To the best of our knowledge, such biosensor for quantitative determination of catechol and phenol has not been reported so far.

## 2. Materials and methods

### 2.1. Chemicals and reagents

Pluronic copolymer P123 (EO20PO70EO20, EO = ethylene oxide, PO = propylene oxide) and tyrosinase (EC 1.14.18.1, from mushroom as lyophilized powder) were purchased from Sigma-Aldrich (USA). Tetraethoxysilane (TEOS), L-cysteine (L-Cys), glutaraldehyde, phenol, catechol, ethylenediamine (EDA), carbon tetrachloride (CTC) and all other chemicals were of analytical grade and used as received. Phosphate buffer solutions (1/15 M PBS) with different pHs were prepared by mixing the stock solution of $KH_2PO_4$ and $Na_2HPO_4 \cdot 12H_2O$. All solutions were prepared with doubly distilled water.

### 2.2. Preparation of ordered mesoporous carbon nitride (MCN) nanocomposites

The mesostructured SBA-15 silica template was synthesized as described previously in our laboratory (Tang et al., 2013). MCN was synthesized using SBA-15 as a template, and carbon tetrachloride was used as a carbon source according to the method reported by Vinu et al. (2005) with slight alterations. A typical procedure was carried out as follows: 0.5 g of mesoporous silica material (SBA-15) was added into a mixture of ethylenediamine (1.35 g) and carbon tetrachloride (3 g). The resulting mixture was refluxed and stirred at 90 °C for 6 h. Then, the obtained dark-brown-colored solid mixture was placed in a drying oven for 12 h, and ground into fine powder. The template-carbon nitride polymer composites were then heat treated in a nitrogen flow of 50 mL per minute

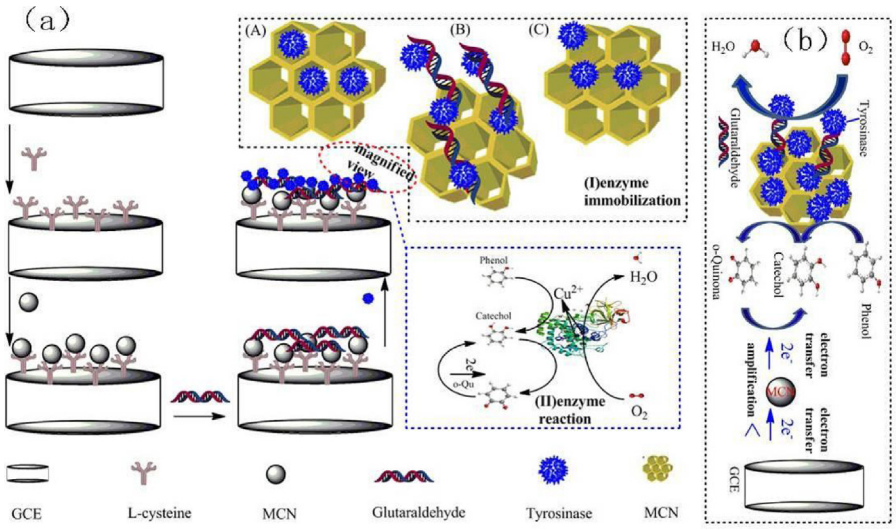


**Scheme 1.** . Schematic illustration of the tyrosinase biosensor preparation and the proposed mechanism for the phenol and catechol electrocatalytic detection (a). Signal transduction and amplification mechanism of biosensor (b).

at 600 °C with a heating rate of 2.0 °C $min^{-1}$ and kept under these conditions for 5 h to carbonize the polymer. The mesoporous carbon nitrides were recovered after dissolution of the silica framework in 5 wt% hydrofluoric acid, by filtration, washed several times with ethanol and dried at 50 °C, and stored for further experiments.

## 3. Results and discussion

### 3.1. Biosensor assembly and catechol, phenol detection mechanism

An ideal biosensor should enable the separation of free and bound targets in a solution phase, further transferring the recognition reaction into detectable signals. In this present work, we designed a tyrosinase biosensor to quantify catechol and phenol simultaneously in compost samples. As illustrated in Scheme 1 the sensing platform was a combination of MCN that acted as a transducer to convert the recognition information into a detectable signal. Initially, the amino modification of MCN could be obtained using L-cysteine by electrochemical method (SI Fig. S-1). It could be seen that there existed voltammetric peaks which maybe resulted from a direct electron transfer from the L-cysteine. As a result, the MCN was fixed on the GCE more firmly. The tyrosinase could be immobilized on the MCN through adsorbing (Scheme 1(A)), cross-linking (Scheme 1(B)) and covalent attachment (Scheme 1(C)), and applied for biosensing using the enzyme activity.

Generally, there exist three aspects which have significant effects on enzyme behavior on biosensors. (i) Enzyme loading efficiency, retention and stability are clearly dependent on the size matching between enzyme and host matrix pore diameter (Tran et al., 2011). In Scheme 1(A), the MCM pore diameter (3.8 nm) promote tyrosinase (2–5 nm size) (Gregory and Srinivasa, 2007) adsorption. (ii) The cross-linking of enzyme aggregates (CLEAs) can form surprisingly stable catalysts (Tran et al., 2011) (Tran et al., 2011). In many cases, CLEAs catalytic activity exceeds that of free enzyme (Roberge et al., 2009; Hara et al., 2008). Here, MCN reacted with glutaraldehyde to supply reactive sites for immobilization of tyrosinase (Scheme 1(B)). (iii) The effects of enzyme-support material interactions have been demonstrated to play significant roles in the loading efficiency of enzymes and their activity, and surface modification of the support could further enhance interactions between the support material and the enzyme, greatly affecting stability, reactivity, and recyclability of enzyme reactors. MCN materials provide aunique opportunity as they contain surface amine groups (Fig. S-3) that can be covalently attached to enzymes. Besides, MCN was functionalized with L-cysteine (Fig. S-3), which can strengthen van der Waals interactions or serve as anchoring points for covalent attachment of enzymes (Tran et al., 2011). As opposed to that of the traditional bioassay for phenols, the whole sensing process in our assay was relatively simple. Moreover, this sensing process effectively facilitated large loading amount of enzyme, increased the possibility of retaining the activity of the tyrosinase, made the tyrosinase more fixed on the biosensor, accelerated the electron transfer from the enzyme-catalyzed redox reaction to electrode surface, and extended its using life as well.

Tyrosinase (or polyphenol oxidase) catalyzes the oxidation of a great variety of hydroxylation of monophenols, diphenols, aromatic amine, etc. The redox reactions of phenol and catechol catalyzed by tyrosinase are described as follows:

$$\text{Phenol} + H_2O + \text{Tyrosinase(oxy)} \rightarrow \text{Catechol} + \text{Tyrosinase(deoxy)} + 2H^+ + 2e^- \quad (1)$$

$$\text{Catechol} + \text{Tyrosinase(oxy)} \rightarrow o - \text{quinone} + \text{Tyrosinase(deoxy)} + 2H^+ + 2e^- \quad (2)$$

$$o - \text{quinone} + 2H^+ + 2e^- \overset{-0.0664\ V}{\Longrightarrow} \text{Catechol} \quad (3)$$

$$\text{Tyrosinase(deoxy)} + O_2 \rightarrow \text{Tyrosinase(oxy)} + H_2O \quad (4)$$

Tyrosinase can catalyze the oxidation of phenol to catechol, catechol to o-quinone (Eqs. (1) and (2)). Under the optimized condition, the o-quinone may be electrochemically reduced to catechol (Eq. (3)). Oxidation process by the tyrosinase, followed by the reduction at the electrode surface, may yield a catalytically amplified current. Therefore, what is occurring at the electrode surface is the reduction of o-quinone to catechol. The proposed mechanism for the phenol and catechol electrocatalytic detection by using the MCN based biosensor is also shown in Scheme 1(b). Briefly, this biosensor can detect catechol and phenol in the presence of both tyrosinase and MCN, and MCN not only facilitates tyrosinase binding but also accelerates electron transfer, thus amplifies electrochemical detection signal. By using this biosensor

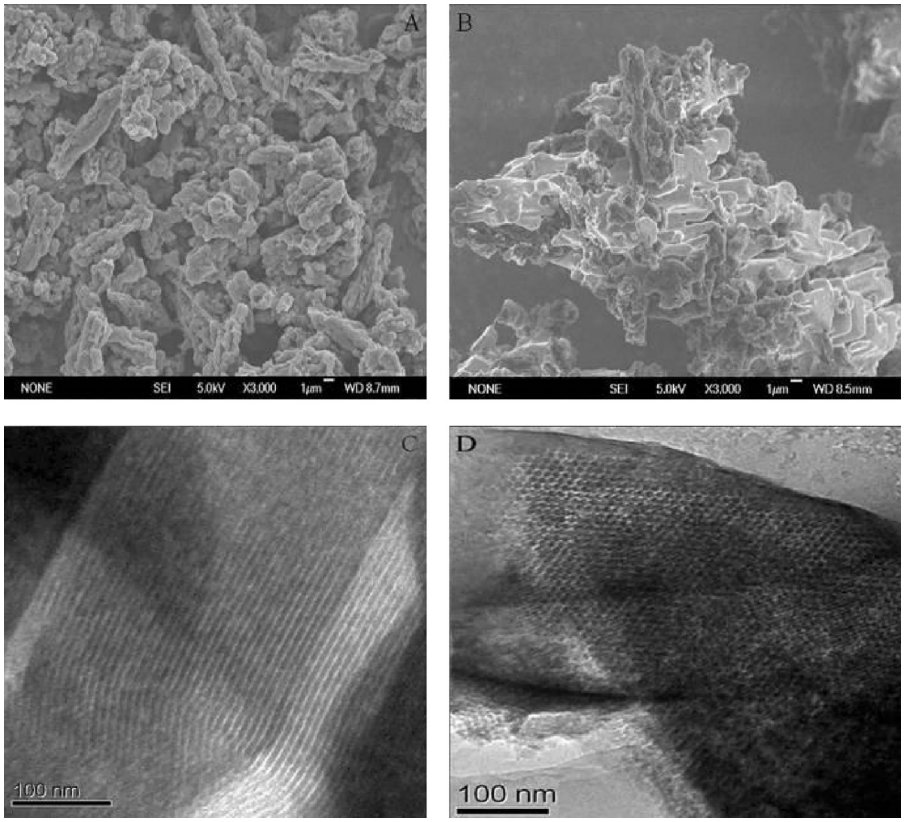


**Fig. 1.** (A) SEM image of MCN. (B) SEM image of MCN/L-cysteine composite. (C) and (D) TEM image of MCN.

the following reactions can be coupled: phenol hydroxylation to catechol occurs first, followed by the catechol oxidation to o-quinone and o-quinone reduction to catechol in the presence of MCN.

### 3.2. Characterization of mesoporous carbon nitride (MCN)

The SEM images of MCN, GCE/L-cysteine/MCN, TEM images of MCN are shown in Fig. 1. As seen in Fig. 1A, the MCN seem like chain structure that were evenly dispersed on the surface of GCE. Fig. 1B presents the SEM image of GCE/L-cysteine/MCN composite. It could be seen that the shape and conformation were a little different from MCN probably due to the role of L-cysteine. The morphological and structural studies of MCN nanoparticles were performed by a transmission electron microscope (TEM). The MCN clearly exhibited highly ordered carbon nanowires (Fig. 1C). When viewed down the direction of only a stripe pattern detected, bright contrast strips on the under-focused image represented images of the pore walls, whereas dark contrast cores represented empty channels. Fig. 1D clearly displays a hexagonal arrangement of the mesopores. The X-ray diffraction (XRD) and $N_2$ adsorption–desorption isotherms for the MCN and SBA-15 are presented in Supporting information (SI) Figs. S-2 and S-3, and the results were described in Supporting information. Besides, the Fourier-transform infrared (FT-IR) spectrum of SBA-15, MCN and MCN-L-cysteine material are shown in SI Fig. S-4, and the results were also described in Supporting information.

### 3.3. Catechol and phenol bioassay

Fig. 2A and B shows the typical current–time plot of the biosensor under the optimized experimental conditions (SI Figs. S-6, S-7 and S-8) after the addition of successive aliquots of phenol or catechol to the PBS under stirring. The biosensing performance presented two response ranges at low and high concentrations for both catechol and phenol. And the electrode showed a rapid and sensitive bioelectrocatalytic response, reaching 95% of the steady-stage current within about 35 and 56 s after addition of catechol and phenol, respectively. The different response times were due to the fact that phenol had to be oxidized to catechol, firstly, which in turn needed to be further oxidized to o-quinone and this last one to be reduced afterwards to catechol in the presence of MCN. However, in the case of catechol detection the first step is omitted. Briefly, the difference in response time depended on the tyrosinase catalytic selectivity for different catechol and phenol compounds. And Carmen et al. (2013) found the similar phenomenon that the response time of catechol was shorter than phenol. As seen in Fig. 2 (inset), it presented the typical calibration curves of the GCE/MCN/Tyr toward phenol and catechol, respectively. Each of the calibration was done three times, and the relative standard deviations (RSD) of the current responses for phenol and catechol were not more than 3.6% and 4.2%, respectively. As seen in Fig. 2A (inset), under the optimal conditions, the cathodic peak current was linear with the phenol concentration ranging from $5.00\times10^{-8}$–$9.5\times10^{-6}$ M

$$y_1 = (681.4709 \pm 4.2770)x_1 + (50.7049 \pm 22.1627) \quad (5)$$

where $y_1$ is the current change (nA), $x_1$ the phenol concentration (μM), and the coefficient is 0.9991. Similarly, as shown in Fig. 2B (inset), the cathodic peak current of catechol increased with its concentration increasing from $5.00\times10^{-8}$ M to $1.25\times10^{-5}$ M. A linear regression equation was obtained as

$$y_2 = (593.1184 \pm 12.3222)x_2 + (303.9409 \pm 85.0428) \quad (6)$$

where $y_2$ is the current change (nA), $x_2$ the catechol concentration (μM), and the coefficient is 0.9881.

On the other hand, according to the generally accepted definition, the GCE/MCN/Tyr biosensor results showed lower detection

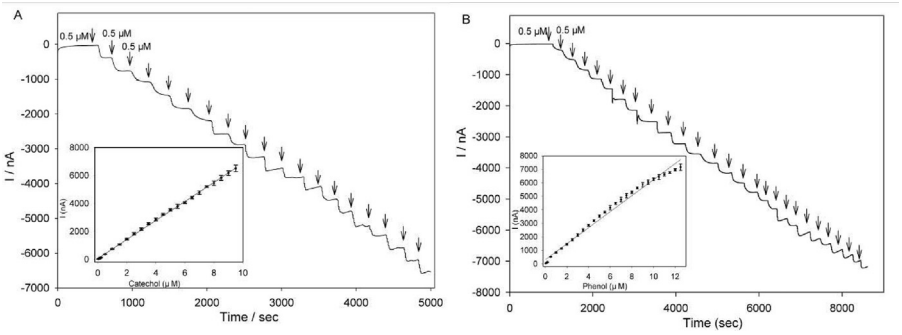


**Fig. 2.** Typical current–time response curves for the successive additions of 0.5 μM of phenol (A) and 0.5 μM of catechol (B); inset: the plot of current response vs. phenol concentration ranging from $5.00 \times 10^{-8}$–$9.50 \times 10^{-6}$ M, catechol concentration between $5.00 \times 10^{-8}$ M and $1.25 \times 10^{-5}$ M. Error bars indicate standard deviations from three replicative tests.

**Table 1**
A comparison of analytical characteristics towards phenol and catechol for tyrosinase biosensors reported in the literature.

| Electrode | Method | Linear range ($\times 10^{-6}$ mol $L^{-1}$) | | LOD ($\times 10^{-8}$ mol $L^{-1}$) | | References |
|---|---|---|---|---|---|---|
| | | Phenol | Catechol | Phenol | Catechol | |
| Tyr/CoPc[a]/CGCE[b] | *i–t* | – | 3.00–863 | – | 45.0 | deAlbuquerque and Ferreira (2007) |
| GCE/Tyr–$Fe_3O_4$–chitosan | *i–t* | 0.0830–70.0 | 0.0830–70.0 | 2.50 | 2.50 | Wang et al. (2008) |
| SPE[c]/MWCNT[d]/Bi/Tissue | *i–t* | 2.00–200 | – | 117 | – | Arben et al. (2010) |
| Tyr–Au/PASE-GO[e]/SPE | *i–t* | – | 0.0830–23.0 | 7.60 | 2.40 | Song et al. (2011) |
| SPE/Tyr/BiNPs | *i–t* | 0.500–100 | 0.500–100 | 6.20 | 2.60 | Carmen et al. (2013) |
| GCE/Tyr/OMC-Au/L-Lysine/Au | DPV | – | 0.400–80.0 | – | 2.5 | Tang et al. (2013) |
| GCE/MCN/Tyr | *i–t* | 0.0500–9.50 | 0.0500–12.5 | 1.024 | 1.500 | This work |

[a] Cobalt (II) phthalocyanine.
[b] Acetylcellulose–graphite composite.
[c] Screen-Printed Electrode.
[d] Multiwalled carbon nanotube.
[e] Succinimidyl ester adsorbing on the graphene oxide.

limit of 10.24 nM and 15.00 nM for catechol and phenol, respectively, which resulted in a current signal that equaled the mean value of background signals plus three times standard deviation of background signals. The sensitivities in the linear calibration regions for low concentration show the following order: 0.6501 A/M (catechol, $n=4$) > 0.6123 A/M (phenol, $n=4$). The difference in sensitivity might depend on the tyrosinase catalytic selectivity for different catechol and phenol. Catechol is a primary substrate of tyrosinase, while phenol could act as secondary substrate of tyrosinase. Compared with the recently reported tyrosinase-modified biosensors on different electrode substrates. As presented in Table 1, the proposed GCE/MCN/Tyr biosensor exhibited improved analytical performances in terms of the detection limit. Moreover, the linear range of the biosensor is also lower than other ones, which suggests that the biosensor is suitable for low concentration detection of phenol and catechol, and the extract samples containing higher concentrations need a simple dilutionin the detection process.

In order to elucidate the lower detection limit, different linear range and sensitivity in the process of phenols detection, and the Michaelis–Menten equation was investigated. Michaelis–Menten analysis of the biocatalyzed oxidation of phenols was carried out using Lineweaver–Burk plots. Lineweaver–Burk equation, a modified version of the Michaelis–Menten equation states that

$$\frac{1}{I}=\frac{1}{I_{\max}}+\frac{K_m}{I_{\max}}\cdot\frac{1}{C} \tag{7}$$

where $I$ is the steady-state current after the addition of substrate, and $I^{-1}$ is the vertical coordinates ($Y$-axis). $I_{\max}$ is the maximum current at saturated substrate concentration, and $C$ in μM is the concentration of substrate (phenol or catechol with the concentration of 0.5–9.5 μM or 0.5–12.5 μM, respectively), and $C^{-1}$ is the abscissa ($X$-axis). $K_m$ is the Michaelis–Menten constant. Using the Lineweaver–Burk equation and representing $I^{-1}$ vs. $C^{-1}$, it is possible to calculate the apparent Michaelis–Menten constant (from the slope) and the $I_{\max}$ (from the intercept). The values of kinetic parameter $K_m$ was obtained by the Lineweaver–Burk plots (Fig. 3). The linear regression analysis for the catechol and phenol indicated that quality of fit was quite good, with $R^2$ values of 0.9794 and 0.9996, respectively. And the RSD values of $I^{-1}$ for phenol and catechol were not more than 3.9% and 4.4%, respectively. The $K_m$ obtained for catechol and phenol were 11.07 μM and 166.80 μM, respectively. The $K_m$ values were lower than that reported for the free enzyme in solution, which was estimated to be 240 μM using catechol as the substrate (Smith and Krueger, 1962), 300 μM using catechol and 700 μM using phenol as the substrate (Espin et al., 2000). The lower $K_m$ values demonstrated that the immobilized Tyr was strongly adsorbed onto the working electrode surface of the GCE modified with MCN, and a good affinity of the enzyme for phenol and catechol is shown.

On the other hand, enzymes on the affinity of the substrate was affiliated with $K_m$. The $K_m$ of catechol (11.07 μM) was lower than that of phenol (166.80 μM) indicating that enzymes on the affinity of catechol was stronger than phenol. And this is the reason that phenol is only capable of acting as secondary substrate of tyrosinase while catechol is a primary substrate for the enzyme. As a result, the sensitivity and detection limit of phenol and catechol were different.

### 3.4. Interference

The specificity of the assay was evaluated using heavy metals ($Mg^{2+}$, $Cu^{2+}$) and other organic compounds, especially hydroquinone. To evaluate the selectivity of the biosensor for catechol,

chronoamperometry response toward $Mg^{2+}$, $Cu^{2+}$, guaiacol, glucose and aniline (each one at 10 times of catechol concentration) and phenol, catechol, hydroquinone was measured (Fig. 4). The degree of interference was calculated according to the following equation:

$$\tau = \frac{I_N}{I_0} \quad (8)$$

where $\tau$ is the percent of interference, $I_0$ stands for the response currents of 0.1 μM catechol or phenol, and $I_N$ stands for the response currents of interferent. From Fig. 4A, it could be seen that $Mg^{2+}$, $Cu^{2+}$, guaiacol, glucose and aniline at 10 times of catechol concentration had little effect on the detection of catechol and their interferences were found to be negligible. After the addition of hydroquinone at 10%, 20% and 30% of catechol concentration continuously, the percent of interference ($\tau$) was 3.84%, 7.81%, and 13.4%, respectively. And the percent of interference changed to 11.5% by adding the same amount of phenol (0.1 μM). The results showed that the interference of hydroquinone to catechol was higher than that of phenol, may be due to the hydroquinone could act as indirect substrate of tyrosinase when catechol was available (Song et al., 2011; Tang et al., 2013), while the reaction of phenol with tyrosinase will be slow under the optimized experimental conditions of catechol (pH 6.98, applied potential −0.0664 V). In general, although hydroquinone at 30% of catechol concentration and the same concentration of phenol had small effect in the process of detection of catechol, the proposed tyrosinase biosensor exhibited the ability to reduce the influences of possible interferences if high concentration of hydroquinone is avoided.

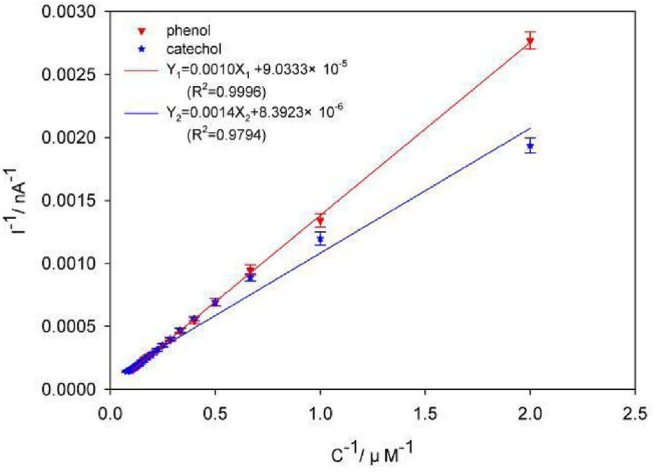


**Fig. 3.** The resulting Lineweaver–Burk plot of catechol and phenol (double-reciprocal plot). Error bars indicate standard deviations from three replicative tests.

From Fig. 4B, it is clearly shown that $Mg^{2+}$, $Cu^{2+}$, guaiacol, glucose, and aniline with 10 times of phenol (0.1 μM) concentration had little effect on the quantification of phenol. And the percent of interference ($\tau$) was only 5.88% after the addition of the same hydroquinone (0.1 μM). Besides, the percent of interference ($\tau$) was 20.8% by adding the same amount of catechol, which might be due to the fact that catechol was a primary substrate for the tyrosinase despite it was under the optimized experimental conditions of phenol (pH 6.98, applied potential −0.0205 V). The results showed that the relative responses obtained from most of these interferents were found to be negligible in the process of detection of phenol under the applied potential of phenol of −0.0205 V. However, a pretreatment was necessary if the concentration of catechol was similar to phenol or higher than phenol in the process of quantification of phenol in real environmental samples, due to the $\tau$ changed to 20.8%.

Briefly, the proposed tyrosinase biosensor exhibited the ability to reduce the influences of possible interferences and provided the potential to selectively determine catechol and phenol levels in compost samples, which could be ascribed to the very low and different applied potentials between them, and the use of tyrosinase. For tyrosinase, catechol is a primary substrate, phenol could act as secondary substrate, while heavy metals ($Mg^{2+}$, $Cu^{2+}$) and other organic compounds, such as hydroquinone, are not a substrate for this enzyme.

### 3.5. Repeatability and reproducibility of the biosensor

The repeatability of the same GCE/MCN/Tyr biosensor was examined by adding catechol in 1/15 M PBS using chronoamperometry, continuously (shown in Fig. S-9). An RSD value was obtained for three successive determinations (<3.192%), which implied a good repeatability of the measurements with no need to apply a complicated pretreatment procedure to the electrode. The reproducibility was also investigated with five different GCEs constructed by the same procedure independently, as presented in Fig. S-10. The RSD was 3.51% for the response current to 0.1 μM catechol, indicating that the fabrication procedure was reliable and the modified GCE had good reproducibility.

### 3.6. Application in compost extracts

Catechol concentration of three compost extract samples was determined by biosensor and HPLC. The compost extracts samples collected need tedious procedures to show no phenol and hydroquinone present (analyzed by HPLC), while simply filtered and diluted when using the method of biosensor. The results of the two methods were approximately the same, shown in Table S-1. Correspondingly, as seen in Table S-2, from the results, it is easy to find that the two methods displayed a good correlation. Consequently, the biosensor

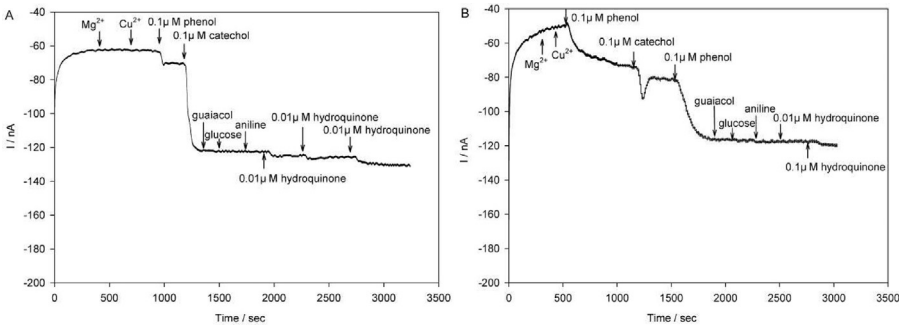


**Fig. 4.** (A) Current–time response curves of GCE/MCN/Tyr with addition of different interfering substances under the optimized experimental conditions of catechol (pH 6.98, applied potential −0.0664 V). (B) Current–time response curve of GCE/MCN/Tyr with addition of different interfering substances under the optimized experimental conditions of phenol (pH 6.98, applied potential −0.0205 V).

offered a simple, fast and sensitive method for catechol and phenol detection with favorable accuracy and specificity.

All these tests provide evidence indicating that the modified electrode had high sensitivity, selectivity, repeatability, and reproducibility which may be ascribed to the following three factors. First, MCN was adsorbed on the electrode surface by linking the –COOH of L-Cys through carboxyl-amino bonding, and a powerful electron tunnel was built on the electrode surface, markedly improving the electric conductivity and reducing the impedance of the electrode (SI Fig. S-5). Second, the use of low concentration L-Cys protected the link between MCN and GCE by forming a film. They could make the MCN film fixed more tightly through its carboxyl-amino as molecular bridge. And this method might extend the using life, repeatability, and reproducibility of the biosensor. The last and the most, with the CN matrix inside the mesopores and the $\pi$–$\pi^*$ electronic transition in the MCN (Vinu et al., 2005), the MCN offered more reaction sites and a good geometrical congruence with the enzyme, then loading more enzymes (Scheme 1), which is important for biosensor performance.

## 4. Conclusion

In summary, we reported the assembly of ordered mesoporous carbon nitride material (MCN) and tyrosinase (Tyr) to develop an enzyme-based biosensor for rapid and sensitive detection of phenol and catechol simultaneously in compost bioremediation samples. The optimized experimental conditions for the operation of the enzyme biosensor, catechol and phenol detection and biosensor assembly mechanism had been studied. The superior sensitivity, stability, and especially selectivity were obtained with obvious advantages for catechol and phenol determination in the real samples of compost extracts. The detection results of the biosensor and the parallel HPLC method were in close propinquity, while the method of biosensor was much simpler, more convenient, rapid and sensitive. Furthermore, it could avoid the interference from turbidity and UV–vis-light-absorbing substances in the detection process in the complex compost system. All of these clearly illustrated that this biosensor offered a possible and economical method for "on-the-spot" monitoring of catechol and phenol in the compost bioremediation system. In addition, it is indicated that the unique MCN and the proposed method presented here could provide new opportunities for the development of other enzyme-based biosensors for analysis of small molecules or pollutants in the biological and environmental fields in the future.

## Supporting information

More details of the apparatus and reagents; characterization of MCN in the XRD, N2 adsorption–desorption isotherms and the FT-IR; characterization of enzyme-based biosensor; optimization of enzyme-based biosensor in pH, coverage of tyrosinase solution, and incubation time for the Glu reaction and the concentration of Glu; the repeatability, reproducibility and long-term stability of the biosensor; sample preparation and analysis of catecholand phenol in compost extracts samples. This material is available free of charge via Internet at http://www.pubs.acs.org.

## Acknowledgments

The study was financially supported by The Young Top-Notch Talent Support Program of China (2012), the National Natural Science Foundation of China (51222805), the Program for New Century Excellent Talents in University from the Ministry of Education of China (NCET-11-0129), Interdisciplinary Research Project of Hunan University, China Scholarship Council (CSC) (2010843195), the Fundamental Research Funds for the Central Universities, Hunan University, Foundation for the Author of Excellent Doctoral Dissertation of Hunan Province, and Hunan Provincial Innovation Foundation For Postgraduate (CX2009B080).

## Appendix A. Supplementary material

Supplementary data associated with this article can be found in the online version at http://dx.doi.org/10.1016/j.bios.2014.05.063.

## References

Apetrei, C., Alessio, P., Constantino, C.J.L., De Saja, J.A., Rodriguez-Mendez, M.L., Pavinatto, F.J., Giuliani Ramos Fernandes, E., Zucolotto, V., Oliveira Jr., O.N., 2011. Biosens. Bioelectron. 26, 2513–2519.
Arben, M., Ulku, A., Serdar., C., Meliha, C., Maria, G., 2010. Electroanalysis 22, 1429–1436.
Canofeni, S., Sario, S.D., Mela, J., Pilloton, R., 1994. Anal. Lett. 27, 1659–1662.
Carmen, C., Mayorga, M., Miquel, C., Maria, G., Josep, R., Arben, M., 2013. Biosens. Bioelectron. 40, 57–62.
Caseli, L., Perinotto, A.C., Vitala, T., Zucolotto, V., Oliveira, O.N., 2009. Langmuir 25, 3057–3061.
deAlbuquerque, Y.T., Ferreira, L.F., 2007. Anal. Chim. Acta 596, 210–221.
Espin, J.C., VarÓn, R., Fenoll, L.G., Gilabert, M.A., García-Ruíz, P.A., Tudele, J., García-anovas, F., 2000. Eur. J. Biochem. 267, 1270–1279.
Fusco, M.D., Tortolini, C., Deriu, D., Mazzei, F., 2010. Talanta 81, 235–240.
Gregory, F.P., Srinivasa, R.R., 2007. Soft Matter 3, 521–527.
Hara, P., Hanefeld, U., Kanerva, L.T., 2008. Mol. Catal. B: Enzym. 50, 80–86.
Hartmann, M., 2005. Chem. Mater. 17, 4577–4593.
Li, Y.F., Liu, Z.M., Liu, Y.L., Yang, Y.H., Shen, G.L., Yu, R.Q., 2006. Anal. Biochem. 349, 33–40.
Liu, L., Guo, L.P., Bo, X.J., Bai, J., Cui, X.J., 2010. Anal. Chim. Acta 673, 88–94.
Lu, L., Zhang, L., Zhang, X., Huan, S., Shen, G., Yu, R., 2010. Anal. Chim. Acta 665, 146–151.
Liu, Y., Qu, X.H., Guo, H.W., Chen, H.J., Liu, B.F., Dong, S.J., 2006. Biosens. Bioelectron. 21, 2195–2201.
Lu, Y., Wen, Z.Y., Jin, J., Cui, Y.M., Wu, M.F., Sun, S.J., 2012. J. Solid State Electrochem. 5, 1863–1866.
Park, S.S., Chu, S.W., Xue, C.F., Zhao, D.Y., Ha, C.S., 2011. J. Mater. Chem. 21, 10801–10807.
Peralta-Zamora, P., Pereira, C.M., Tiburtius, E.R.L., Moraes, S.G., Rosa, M.A., Minussi, R.C., Duran, N., 2003. Appl. Catal. B: Environ. 42, 131–144.
Qu, Y., Ma, M., Wang, Z.G., Zhan, G.Q., Buhai, Li, Wang, X., Fang, H.F., Zhang, H.J., Li, C.Y., 2013. Biosens. Bioelectron. 44, 85–88.
Ramiz, S.J.A., Maryna, O., Silvana, A., 2012. Anal. Chem. 84, 9729–9737.
Roberge, C., Amos, D., Pollard, D., Devine, P., 2009. J. Mol. Catal. B: Enzym. 56, 41–45.
Ryoo, R., Joo, S.H., Jun, S., 1999. J. Phys. Chem. B. 103, 7743–7746.
Shan, D., Zhu, M., Han, E., Xue, H., Cosnier, S., 2007. Biosens. Bioelectron. 23, 648–654.
Smith, J.L., Krueger, R.C., 1962. J. Biol. Chem. 237, 1121–1128.
Song, W., Li, D.W., Li, Y.T., Li, Y., Long, Y.T., 2011. Biosens. Bioelectron. 26, 3181–3186.
Švitel, J., Miertuš, S., 1998. Environ. Sci. Technol. 32, 828–832.
Tang, L., Zhou, Y.Y., Zeng, G.M., Li., Z., Liu, Y.Y., Zhang, Y., Chen, G.Q., Yang, G.D., Lei, X. X., Wu, M.S., 2013. Analyst 138, 3552–3560.
Tang, L., Zeng, G.M., Liu, J.X., Xu, X.M., Zhang, Y., Shen, G.L., Li, Y.P., Liu, C., 2008. Anal. Bioanal.Chem. 391, 679–685.
Topping, D.C., Bernard, L.G., O'Donoghue, J.L., English, J.C., 2007. Food Chem. Toxicol. 45, 70–78.
Tran, I., Daniel, N., Kenneth, J., Balkus, J., 2011. ACS Catal 1, 956–968.
Tsai, Y.C., Chiu, C.C., 2007. Sens. Actuators B 125, 10–16.
Vinu, A., Ariga, K., Mori, T., Takashi, Hishita, S., Golberg, D., Bando, Y., 2005. Adv. Mater. 17, 1648–1652.
Wang, H.F., Wu, Y.Y., Yan, X.P., 2013. Anal. Chem. 85, 1920–1925.
Wang, S.F., Tan, Y.M., Zhao, D.M., Liu, G.D., 2008. Biosens. Bioelectron. 23, 1781–1787.
Wei, J., Zhou, D.D., Sun, Z.K., Deng, Y.H., Xia, Y.Y., Zhao, D.Y., 2013. Adv. Funct. Mater. 23, 2322–2328.
Wu, J., Liao, L., Yan, W.S., Xue, Y., Sun, Y.F., Yan, X., Chen, Y.X., Xie, Y., 2012. ChemSusChem 5, 1207–1212.
Xin, J., Veerappan, V., Balasubramanian, Sakthivel, T.S., Dhanashri, P.S., Murugulla, A.C., Lu, G.Q., Ajayan, V., 2009. Angew. Chem. 121, 8024–8027.
Yildiz, H.B., Toppare, L., Gursel, Y.H., Yagci, Y., 2006. Enzyme Microb. Technol. 39, 945–948.
Zhang, Y., Zeng, G.M., Tang, L., Li, Y.P., Chen, L.J., Pang, Y., Li, Z., Feng, C.L., Huang, G. H., 2011. Analyst 136, 4204–4210.
Zhao, J.W., Zhi, J.F., Zhou, Y.L., Yan, W.B., 2009. Anal. Sci. 25, 1083–1088.
Zhou, M., Shang, L., Li, B.L., Huang, L.J., Dong, S.J., 2008. Biosens. Bioelectron. 24, 442–447.